CrossMark

Clausenidin from *Clausena excavata* induces apoptosis in hepG2 cells via the mitochondrial pathway

Peter M. Waziri[a,b,*], Rasedee Abdullah[c], Swee Keong Yeap[d], Abdul Rahman Omar[d],
Ahmad Bustamam Abdul[a], Nur Kartinee Kassim[e], Ibrahim Malami[a],
Thiruventhan Karunakaran[e], Mustapha Umar Imam[f]

[a] *MAKNA Cancer Research Laboratory, Institute of Bioscience, University Putra Malaysia, Serdang, Selangor, Malaysia*
[b] *Department of Biochemistry, Kaduna State University, Main Campus, PMB 2336 Kaduna, Nigeria*
[c] *Department of Veterinary Pathology and Microbiology, Faculty of Veterinary, University Putra Malaysia, Serdang, Selangor, Malaysia*
[d] *Laboratory of Vaccine and Therapeutics, Institute of Bioscience, University Putra Malaysia, Serdang, Selangor, Malaysia*
[e] *Department of Chemistry, Faculty of Science, University Putra Malaysia, Serdang, Selangor, Malaysia*
[f] *School of Public Health, Zhengzhou University, Zhengzhou City, Henan Province, PR China*

ARTICLE INFO

ABSTRACT

Ethnopharmacological relevance: *Clausena excavata* Burm.*f.* is used locally in folk medicine for the treatment of cancer in South East Asia.
Aim of the study: To determine the mechanism of action of pure clausenidin crystals in the induction of hepatocellular carcinoma (hepG2) cells apoptosis.
Materials and methods: Pure clausenidin was isolated from *Clausena excavata* Burm.*f.* and characterized using ^{1}H and ^{13}C NMR spectra. Clausenidin-induced cytotoxicity was determined by MTT assay. The morphology of hepG2 after treatment with clausenidin was determined by fluorescence and Scanning Electron Microscopy. The effect of clausenidin on the apoptotic genes and proteins were determined by real-time qPCR and protein array profiling, respectively. The involvement of the mitochondria in clausenidin-induced apoptosis was investigated using MMP, caspase 3 and 9 assays.
Results: Clausenidin induced significant ($p < 0.05$) and dose-dependent apoptosis of hepG2 cells. Cell cycle assay showed that clausenidin induced a G2/M phase arrest, caused mitochondrial membrane depolarization and significantly ($p < 0.05$) increased expression of caspases 3 and 9, which suggest the involvement of the mitochondria in the apoptotic signals. In addition, clausenidin caused decreased expression of the anti-apoptotic protein, Bcl 2 and increased expression of the pro-apoptotic protein, Bax. This finding was confirmed by the downregulation of Bcl-2 gene and upregulation of the Bax gene in the treated hepG2 cells.
Conclusion: Clausenidin extracted from *Clausena excavata* Burm.*f.* is an anti-hepG2 cell compound as shown by its ability to induce apoptosis through the mitochondrial pathway of apoptosis. Clausenidin can potentially be developed into an anticancer compound.

1. Introduction

Clausena excavata Burm. *f.* is a wild shrub from the *Rutaceae* family found predominantly in South and Southeast Asia (Huang et al., 1997; Manosroi et al., 2004). The plant commonly is known as *Cherek Hitam* in Malaysia and *San Soak* in Thailand (Manosroi et al., 2004).

The leaves, twigs, and barks of *C. excavata* have long been used in Asian folk medicine (Wu and Furukawa, 1982; Takemura et al., 2000). In Thailand, *C. excavata* extracts are traditionally used in the treatment of cancers (Perry and Metzger, 1980; Manosroi et al., 2004; Arbab et al., 2013). Other uses of the extracts include for the treatment of colds, dermatopathy, snake bites, malaria, HIV, and abdominal
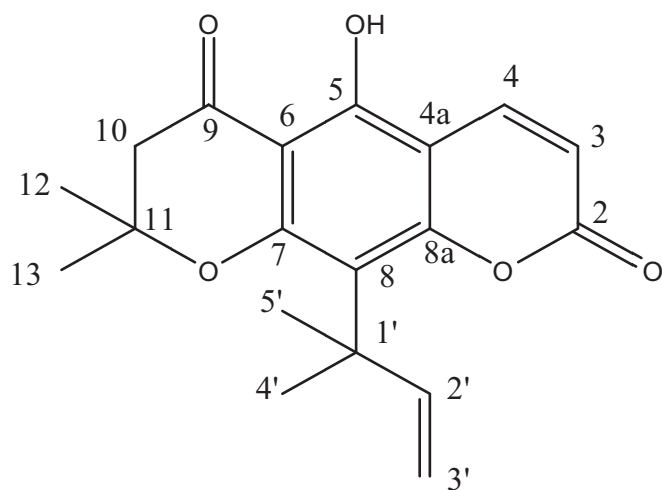
Fig. 1. Chemical structure of clausenidin.

pains (Wu et al., 1994; Kongkathip et al., 2005).

Coumarins and carbazole alkaloids are the major components of *C. excavata*. The coumarins are classified, according to chemical structure, as simple coumarins, furanocoumarins, pyranocoumarins, biscoumarins, triscoumarins, and coumarino lignans. Clausenidin (Fig. 1), a member of the pyranocoumarin family, was shown to cause significant cytotoxicity to several cell lines (Su et al., 2009).

Liver cancer is the leading cause of cancer deaths after colon and lung cancers. According to the World Health Organization estimates for 2012, liver cancer alone accounted for 745,000 deaths worldwide (WHO, 2015). Liver cancer is the leading cause of cancer deaths among men and the sixth leading cause of death among women. Over 80% of liver cancer deaths occur in developing countries and the disease is becoming more rampant in Asia and sub-Saharan Africa than in other regions of the world (Bakiri and Wagner, 2013). Liver cancers occur in various histological forms with hepatocellular carcinoma (HCC) as the most dominant form accounting for 70–85% of all liver tumors (Ferlay et al., 2010; Nordenstedt et al., 2010). Therapeutic options for liver tumors are limited and survival after diagnosis is poor (Bakiri and Wagner, 2013) because the tumor is relatively insensitive to current chemotherapeutics.

Natural products may provide the much needed effective alternative therapeutic compounds with minimal side-effects. Among anticancer compounds of natural origin are flavonoids, polyphenols, and chalcones that have been shown to exhibit in vitro effects against hepG2, HL60 and MDA-MB-231 cell lines. These compounds do not only cause cancer cell toxicity but caused sustained growth inhibitory effects (Fahey and Stephenson, 2002; Tuchinda et al., 2002; Yun et al., 2006; Jing et al., 2010; Isa et al., 2013; Zhang et al., 2014).

Xanthyletin, dentatin, clausenolide 1-methyl ether, and clausenarin isolated from *C. excavata* have also been screened and found to be toxic to several cancer cell lines (Sharif et al., 2013). The current study aimed to determine the effect of clausenidin on the HepG2 cell line. This study, for the first time, describes the toxic effect of clausenidin on hepG2 cells and the mechanism associated with its anti-cancer cell effect.

2. Material and methods

2.1. Plant material collection

Fresh roots of *Clausena excavata* Burm.*f.*, identified by Dr Shamsul Khamis, were collected from the Agricultural park, Institute of Bioscience, University Putra Malaysia. A voucher identification number of 2991/16 was assigned to the plant. Approximately 2 kg of the root were cut into thin slices and air-dried for two weeks. The dried sample was ground to fine powder prior to extraction.

2.2. Extraction and isolation of compound

The ground powder was extracted with analytical grades chloroform and methanol at room temperature. The ground powder was soaked in 10 L chloroform for 3 days and sieved with a 0.45 µm filter paper to collect the extract. The remaining residue was brought to dryness and soaked in 10 L of methanol for another 3 days followed by sieving to collect the extract. The crude extract was concentrated in a rotary evaporator at 45 °C under reduced pressure to obtain the dried extract before further purification. The yield of the extracts were calculated as follows:

Yield (%)=(Weight of extract/weight of fresh plant)×100.

2.3. Column and thin layer chromatography

The chloroform extract was chosen for further purification since it was found to be more cytotoxic than the methanolic extract. Chromatography was performed on a glass column (36×3.5 cm) packed with silica gel of particle size 0.04–0.06 mm. A mixture of hexane-ethyl acetate of increasing polarities was used for the column elution (mobile phase). More than 20 fractions were eluted and subjected to thin layer chromatography (0.25 mm thick plate) (Merck). Fractions 10–16 produced similar TLC profiles and melting points of 135–137 °C; thus they were pooled and concentrated in a rotary evaporator at 45 °C before purification.

2.4. Identification and characterization of clausenidin

The Electron Impact Mass Spectra (EIMS) was recorded on Shimadzu GCMS-QP5050A spectrometer. ^{1}H NMR spectra were

Table 1
Gene name and sequences of primers used in the multiplex panel.

Gene name	Forward sequence	Reverse sequence
Bax	AGGTGACACTATAGAATAGCAAACTGGTGCTCAA	GTACGACTCACTATAGGGAAACCACCCTGGTCTTG
Bcl-2	AGGTGACACTATAGAATACTGTGGATGACTGAGTACCT	GTACGACTCACTATAGGGATCAGAGACAGCCAGGAG
Apaf-1	AGGTGACACTATAGAATACATACTCTTTCACCAGATCA	GTACGACTCACTATAGGGAACAAGTTCTGTTTTTGCTTT
JNK	AGGTGACACTATAGAATACAGAAGCTCCACCACCAAAGAT	GTACGACTCACTATAGGGAGCCATTGATCACTGCTGCAC
Cyt c	AGGTGACACTATAGAATAGAGCGAGTTTGGTTGC	GTACGACTCACTATAGGGAAAATCTTCTTGCCTTTCTC
Caspase 3	AGGTGACACTATAGAATATGTAGAAGAGTTTCGTGAGT	GTACGACTCACTATAGGGAGAGTTTTCAGTGTTCTCCAT
Caspase 9	AGGTGACACTATAGAATAGCTGGTGGAAGAGCTG	GTACGACTCACTATAGGGACTCTAAGCAGGAGATGAACA
β-actin	AGGTGACACTATAGAATAGATCATTGCTCCTCCTGAGC	GTACGACTCACTATAGGGAAAAGCCATGCCAATCTCATC

The β-actin gene was used for normalization. Reverse transcription (RT) and PCR were done according to manufacturer's instructions; RT reaction was at 48 °C for 1 min; 37 °C for 5 min; 42 °C for 60 min; 95 °C for 5 min; then held at 4 °C, while PCR conditions were as follows: initial denaturation at 95 °C for 10 min, followed by two-step cycles of 94 °C for 30 s and 55 °C for 30 s, ending in a single extension cycle of 68 °C for 1 min. Bax=Bcl-2-associated X protein; Bcl-2=B cell lymphoma 2; Apaf-1=Apoptotic protease activating factor 1; JNK=c-Jun N-terminal kinases; Cyt C=cytochrome complex; Caspase 3=Cysteine aspartic acid protease 3; Caspase 9=Cysteine aspartic acid protease 9.
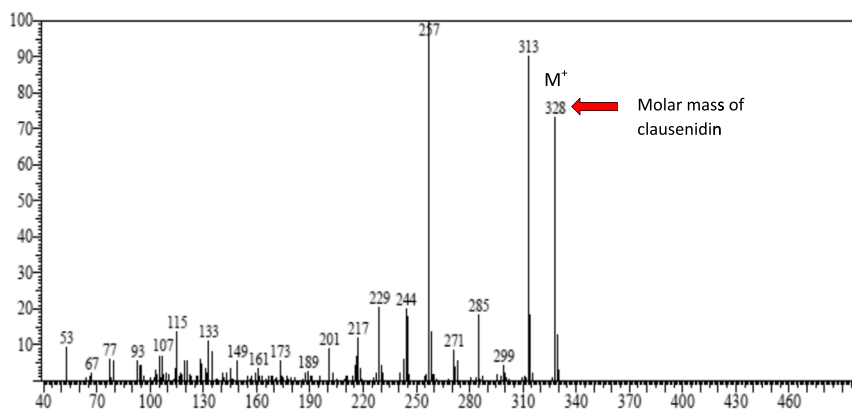
Fig. 2. EIMS spectrum of purified clausenidin.

Table 2
^{1}H, ^{13}C and HMBC NMR Data for clausenidin in CDCl$_3$ (500 and 125 MHz; respectively, δ in ppm, J in Hz).

| NO	δH	δC	HMBC
1			
2		160.6	
3	6.11 (d, J=9.5 Hz, 1 H)	110.6	C-2 (^2J), C-4a (^3J)
4	7.99 (d, J=10 Hz,1 H)	138.5	C-2 (^3J), C-5 (^3J)
4a		103.1	
5	12.94	159.9	C-4a (^3J), C-5 (^2J), C-6 (^3J)
6		103.9	
7		158.9	
8		114.4	
8a		158.9	
9		198.2	
10	2.72 (s, 2H)	47.6	C-6, (^3J), C-9 (^2J), C-11 (^2J), C-12 (^3J), C-13 (^3J)
11		80.0	
12	1.46 (s, 3H)	26.4	C-9 (^4J), C-10 (^3J), C-11 (^2J), C-13 (^3J)
13	1.46 (s, 3H)	26.4	C-9 (^4J), C-10 (^3J), C-11 (^2J), C-12 (^3J)
1'		40.9	
2'	6.19 (dd, J=17 and 9.5 Hz, 1H)	149.5	C-1' (^2J), C-4' (^3J), C-5'(^3J), C-8 (^3J)
3'	4.85 (dd, J=17 and 10 Hz, 2H)	108.3	C-1' (^3J), C-2' (^2J),
4'	1.59 (s, 3H)	29.4	C-1' (^2J), C-2'(^3J), C-3' (^4J), C-8 (^3J)
5'	1.59 (s, 3H)	29.4	C-1' (^2J), C-2' (^3J), C-3' (^4J), C-8 (^3J)
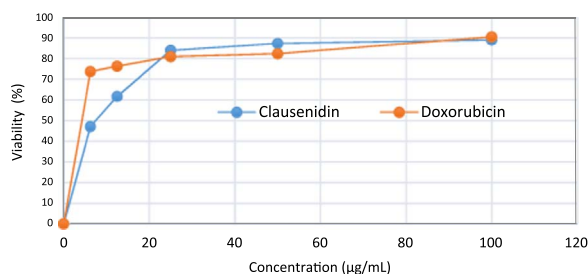
Fig. 3. Viability of hepG2 cells after treating with clausenidin for 72 h. The IC$_{50}$ of clausenidin and doxorubicin is 7.7 ± 0.29 μg/mL and 5.3 ± 2.19 μg/mL respectively as determined from the plot.

recorded on Varian NMR system (500 MHz, USA). ^{13}C spectra were obtained on the same Varian NMR instrument operating at 125 MHz while the melting point was obtained using a Barnstead melting point apparatus.

2.5. Cell viability assay

Human hepatocellular carcinoma (HepG2) cells were obtained from the American Type Culture Collection (ATCC, Va, USA). The cells were maintained in RPMI-1640 medium supplemented with 10% fetal bovine serum (FBS). Approximately 5×10^3 cells were seeded into each well of a 96-well plate and incubated overnight. The cells were then treated separately with increasing concentrations of clausenidin and doxorubicin (positive control). After 72 h, 5 mg/mL MTT solution were added to determine cell viability as described previously (Syama et al., 2013). The results were expressed as percent cytotoxicity at 72 h exposure to test agents.

2.6. Morphological assessment of apoptotic cells by acridine orange (AO) and propidium iodide (PI) double staining

Clausenidin-induced hepG2 cell death was monitored by acridine orange (AO) and propidium iodide (PI) double-staining method according to standard procedures. The cells (10^5 cells/well) were seeded in a 6-well plate and incubated overnight. The cells were then treated for 24 h with 5, 15, and 30 μg/mL clausenidin, harvested, and washed with PBS, centrifuged at $1000 \times g$ for 5 min, and the supernatant discarded. The washing procedure was repeated twice to remove traces of media. Ten microliters of fluorescent dyes containing 10 mg/mL AO and 10 mg/mL PI were added to the cell pellet. A drop of freshly stained cell suspension was placed on a glass slide, covered with a cover slip and observed under fluorescent microscopy within 30 min before the fluorescence fades.

2.7. Scanning electron microscopy

To prepare for scanning electron microscopy (SEM), the hepG2 cells were seeded at a density of 10^6 cells/T-25 mL flask and incubated overnight. The cells were then treated with the IC$_{50}$ (7.7 μg/mL) of clausenidin for 48 and 72 h while those treated with 0.1% (v/v) DMSO served as the negative control. The cells were harvested and washed with PBS before fixing with 4% glutaraldehyde for 24 h followed by 1% osmium tetroxide at 4 °C for 2 h. The cells were then washed three times with 0.1 M sodium cacodylate buffer and dehydrated with increasing acetone concentration from 30% to 99.9%. The cells were then coated with gold in a sputter coater before viewing under the JSM 6400 scanning microscope.

2.8. Cell cycle analysis by flow cytometry

The hepG2 cells were seeded at 10^6 cells/T-25 mL flask in RPMI media and incubated overnight and then treated with the IC$_{50}$ (7.7 μg/mL) of clausenidin for 24, 48 and 72 h. Cell treated with 0.1% (v/v) DMSO served as the negative control. Harvested cells were washed
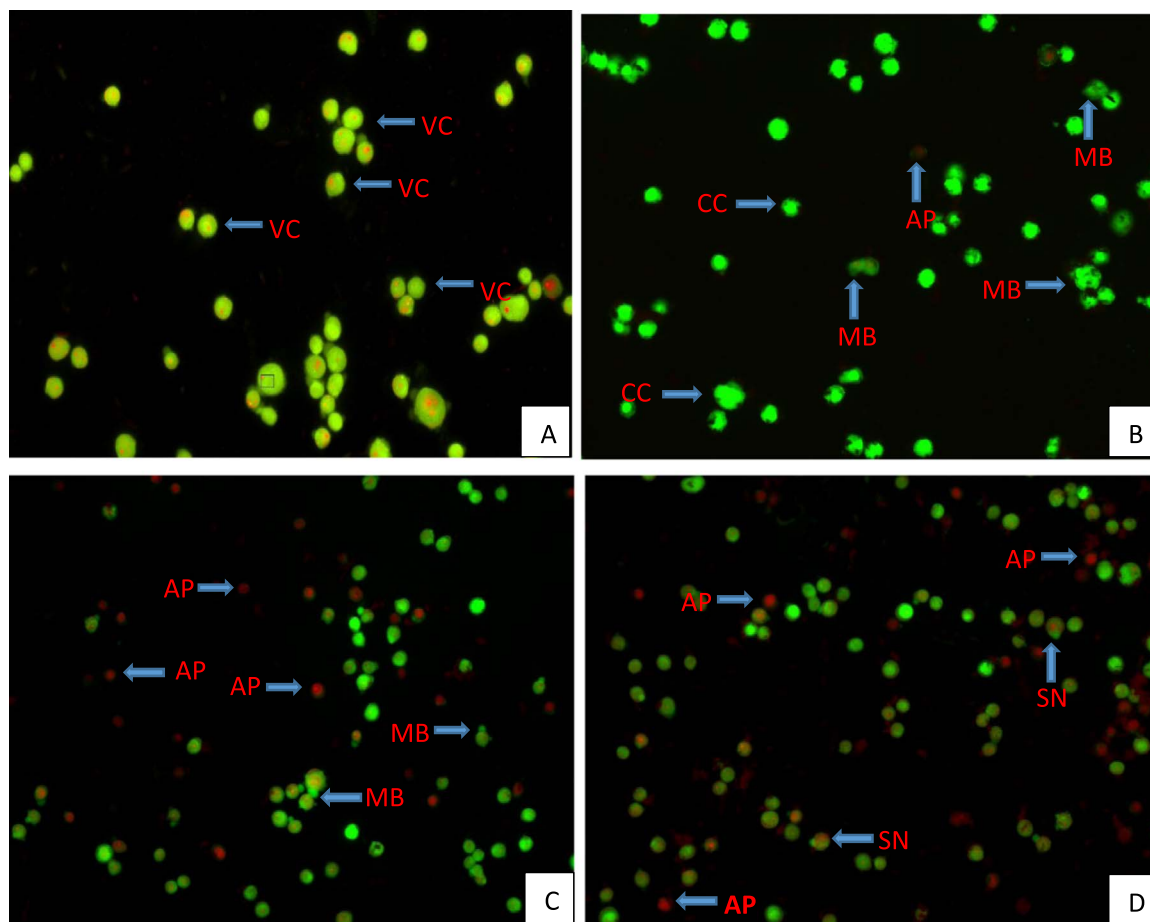
Fig. 4. Acridine orange and propidium iodide-stained hepG2 cells treated with clausenidin for 24h (A) Untreated cells and cells treated with (B) 5 (C) 15, and (D) 30 μg/mL clausenidin. VC=viable cells, MB=membrane blebbing, CC=chromatin condensation, AP=apoptosis, and SN=secondary necrosis. 100× Magnification.

with PBS. Cell cycle assay was performed using BD cell cycle reagent (CycleTest™ Plus DNA reagent kit, Becton Dickinson, Belgium) and flow cytometry.

2.9. Annexin V assay

HepG2 cells were seeded at 2×10^5cells/T-25 mL flask in RPMI media and incubated overnight before treating with the IC_{50} (7.7 μg/mL) of clausenidin or 0.1% (v/v) DMSO (control) for 24, 48 and 72 h. The cells were harvested, washed with PBS and subjected to Annexin V assay using the FITC annexin V assay kit (BD Pharmingen, USA) and flow cytometry.

2.10. Mitochondrial membrane potential (MMP) assay

Mitochondrial membrane potential assay was performed to determine mitochondrial membrane integrity. HepG2 cells were seeded in a 6-well plate at 5×10^5 cells/well, incubated overnight and then treated with 5, 15, 30, and 40 μg/mL clausenidin. The negative control cells were treated with 0.1% (v/v) DMSO. The assay was performed using the BD™ Mitoscreen kit (BD biosciences, US) and flow cytometry.

2.11. Caspases 3 and 9 assays

Caspases 3 and 9 activities were determined using the colorimetric method (Genscript Colorimetric Assay kit, USA). Cells were initially seeded in a 6-well plate at 10^6 cells/well overnight. The cells were treated for 24 h with 5, 15, 30, 40 and 50 μg/mL clausenidin and caspases 3 and 9 assays performed. Negative control cells were treated

with 0.1% (v/v) DMSO. After completion of reaction, the plates were read on microplate reader at 405 nm.

2.12. RNA isolation

RNA extraction was basically done to determine gene expression. HepG2 cells in a 6-well plate containing 10^6 cells/well were treated with the IC_{50} (7.7 μg/mL) of clausenidin and 0.1% DMSO (negative control) for 12 and 24 h. After detachment with trypsin the cells were harvested and washed with PBS. RNA was extracted using the Total RNA extraction kit (GF-1 TRE kit, Vivantis technologies), and quantified using a nanodrop spectrophotometer at 260 nm.

2.13. RT-qPCR

The reverse transcriptase quantitative PCR (RT-qPCR) was carried out according to the GenomeLab GeXP Kit (Beckman Coulter, USA) protocol, in an XP Thermal Cycler (Bioer Technology, Germany). PCR products were finally analyzed in the GeXP genetic analysis system and the results normalized using the Express Profiler software. The primers for the genes of interest and housekeeping gene (Table 1) were designed on the NCBI website and purchased from Biosune (Shanghai, China), while the internal control (Kanr) from Beckman Coulter (USA).

2.14. Protein profile array

Apoptosis-related protein profile array analysis (Table 3) was done to determine the effect of clausenidin treatment on hepG2 cells.
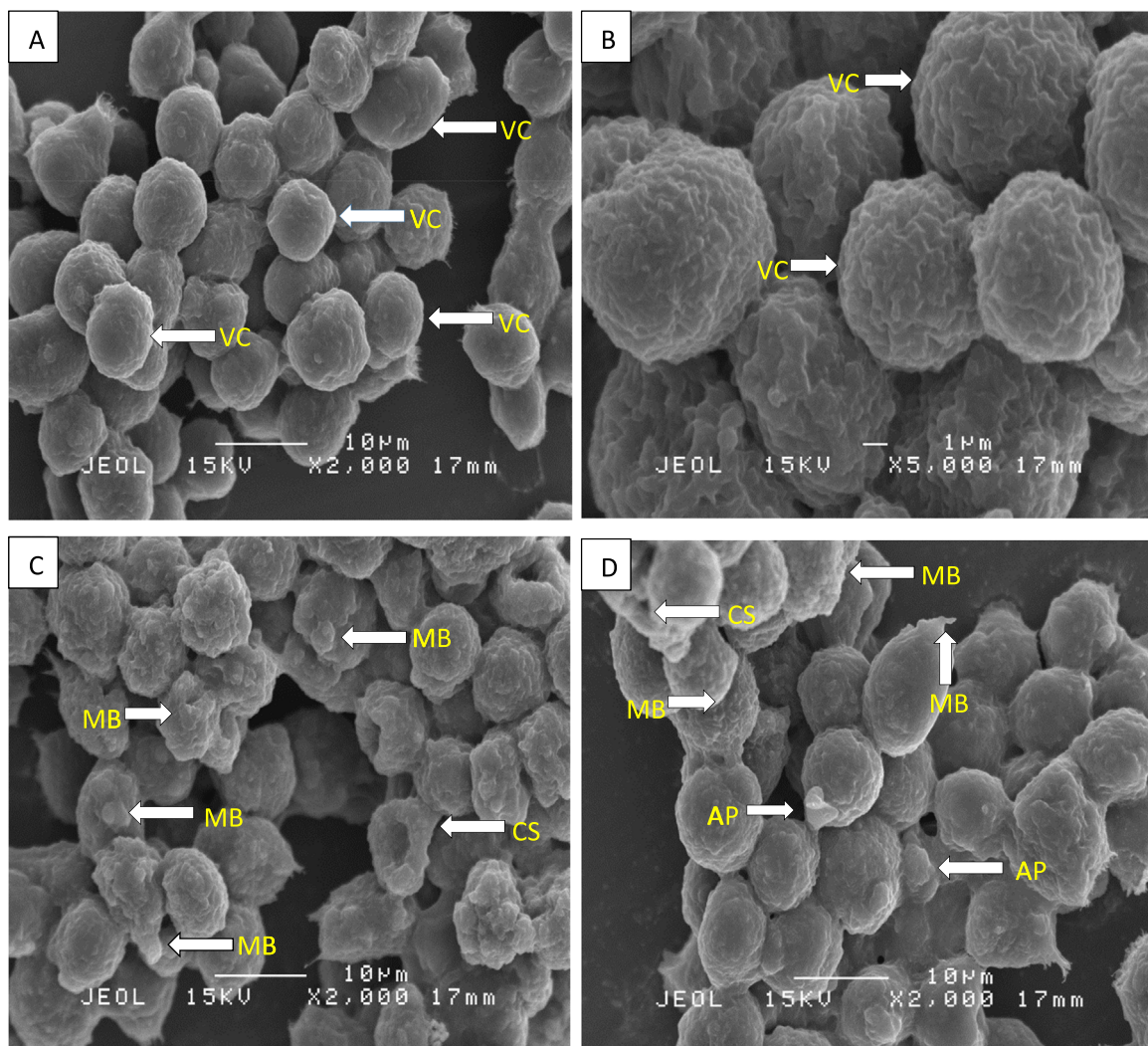
Fig. 5. HepG2 cells treated with 7.7 µg/mL clausenidin. (A and B) Intact control cells, (C) membrane blebbing and cytosolic shredding observed after 48 h, (D) membrane blebbing, cytosolic shredding, and apoptotic body formation after 72 h. VC=viable cells, MB=membrane blebbing, CS=cytosolic shredding, AP=apoptotic body.

Determination of HepG2 cell protein expression was done using a proteome profiler antibody array kit (R & D systems, USA). The cells were seeded overnight at a density of 10^6 cells/well and treated with the IC_{50} (7.7 µg/mL) of clausenidin for 24 h. The negative control cells were treated with 0.1% (v/v) DMSO. Proteins were quantified using the Bradford's assay. Primary antibody-coated membranes were incubated with 200–400 µg/mL protein samples overnight at 4 °C. The membranes were then washed with wash buffer before incubating with the secondary antibody conjugated with horse radish peroxidase, for 30 min on a rocking platform. The membranes were again washed and the chemireagent mixture slowly added to allow for an even spread over the membrane surface. The images were then captured on a chemidoc (Biorad, USA) imaging system and analyzed using the *image lab* software 5.

2.15. Statistical analysis

Data are presented as mean ± standard deviation. One-way Analysis of Variance (ANOVA) using SPSS 22 software (SPSS Inc, Chicago IL, USA) was used to determine significant difference between means at 95% confidence interval ($p < 0.05$).

3. Results

3.1. Purification and characterization of clausenidin

The yield of chloroform extract was 0.3%. The EIMS spectrum (Fig. 2) gave a molecular peak at *m/z* 328 confirming the molar mass of clausenidin reported by a previous study (Wu, 1982). The melting point of 135–137 °C and the NMR data (Table 2) of clausenidin obtained in this report are similar to that reported earlier (Wu, 1982; Huang et al., 1997).

3.2. Cell viability and cytotoxicity assay

Clausenidin-induced hepG2 cell death was dose-dependent. The IC_{50} of pure clausenidin on hepG2 cells at 72 h was 7.7 ± 0.29 µg/mL. Doxorubicin-induced hepG2 cell toxicity was also dose-dependent with IC_{50} of 5.3 ± 2.19 µg/mL (Fig. 3).

3.3. Fluorescent microscopy

The hepG2 cell death increased with increase of clausenidin concentration (Fig. 4). Treated hepG2 cells show distorted morphology characterized by membrane blebbing and chromatin condensation, which are features of apoptosis. In addition, some of the cells went into secondary necrosis.
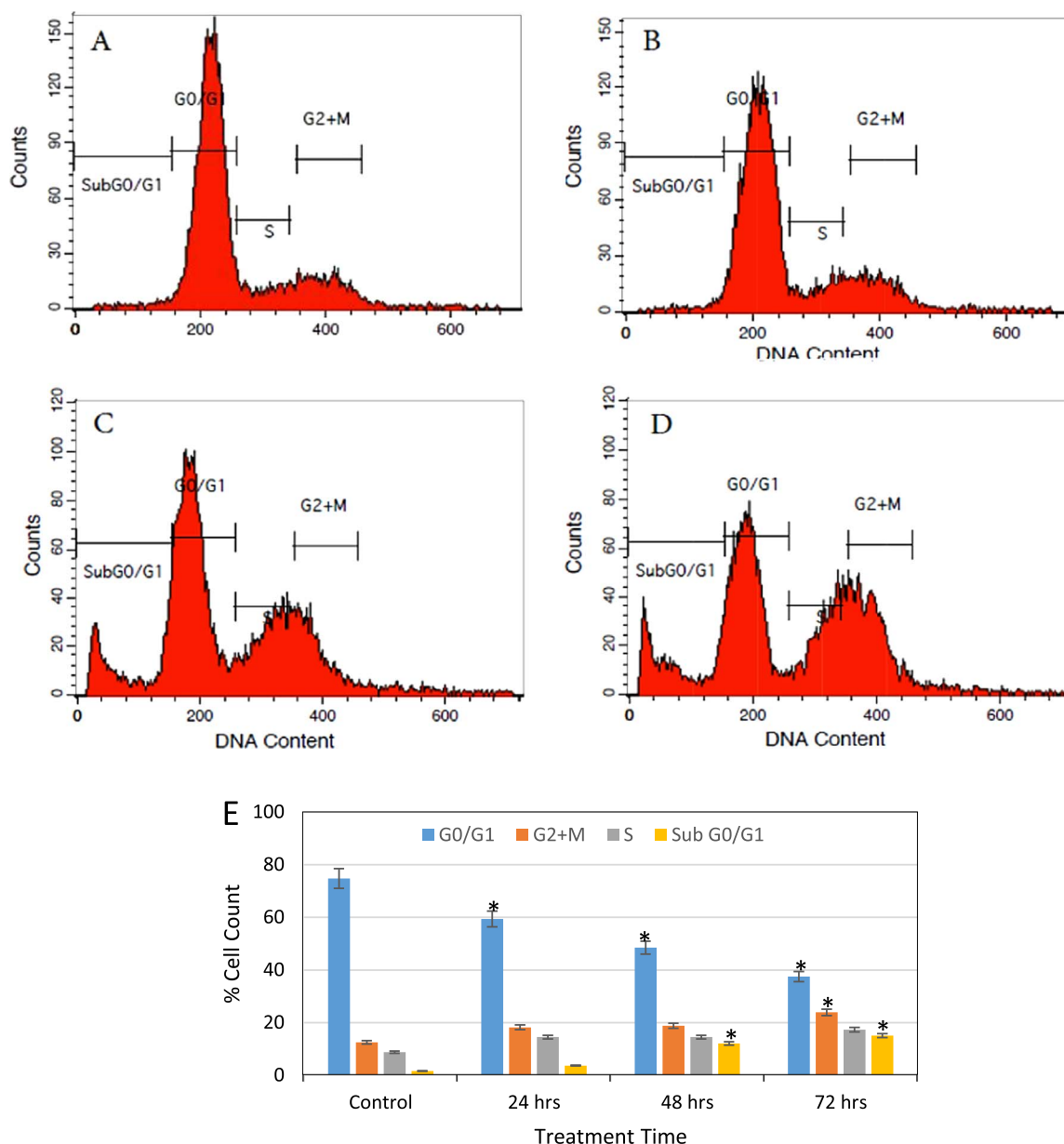
Fig. 6. DNA content of hepG2 cells treated with 7.7 µg/mL clausenidin. (A) Untreated control, and at (B) 24, (C) 48, and (D) 72 h of treatment. (E) Distribution of cells according to cell cycle phase. *For each cell cycle phase, means significantly ($p < 0.05$) different from control.

3.4. Scanning electron microscopy (SEM)

Fig. 5 shows early apoptosis of hepG2 cells characterized by membrane blebbing. With treatment time, cytosolic shredding increased in intensity.

3.5. Cell cycle analysis

Cell cycle analysis, showed that hepG2 cells treated with clausenidin entered a G2/M phase arrest (Fig. 6). Consequently, the proportion of cells in the resting G0/G1 phase decreased significantly ($p < 0.05$) while those in subG0/G1 (apoptotic cells) increased significantly ($p < 0.05$) after 72 h of clausenidin treatment.

3.6. Annexin V assay

The DNA content, as a measure of cell viability, showed significant ($p < 0.05$) decrease in viable cells while there were significant ($p < 0.05$) increases in early and late apoptotic cells after 48 and 72 h of

clausenidin treatment (Fig. 7).

3.7. Mitochondrial membrane potential

The fluorescent intensity produced upon treating hepG2 cells with clausenidin is a measure of mitochondrial membrane potential (MMP). Clausenidin treatment caused membrane depolarization of the hepG2 cells (Fig. 8). The rate of mitochondrial membrane depolarization is directly proportional to the concentration of clausenidin used in the treatment.

3.8. Caspases 3 and 9 assay

Fig. 9 shows that clausenidin, as indicated by the fold change, induces a significant ($p < 0.05$) increase in hepG2 cell caspases 3 and 9 activities that is proportional to clausenidin concentration.
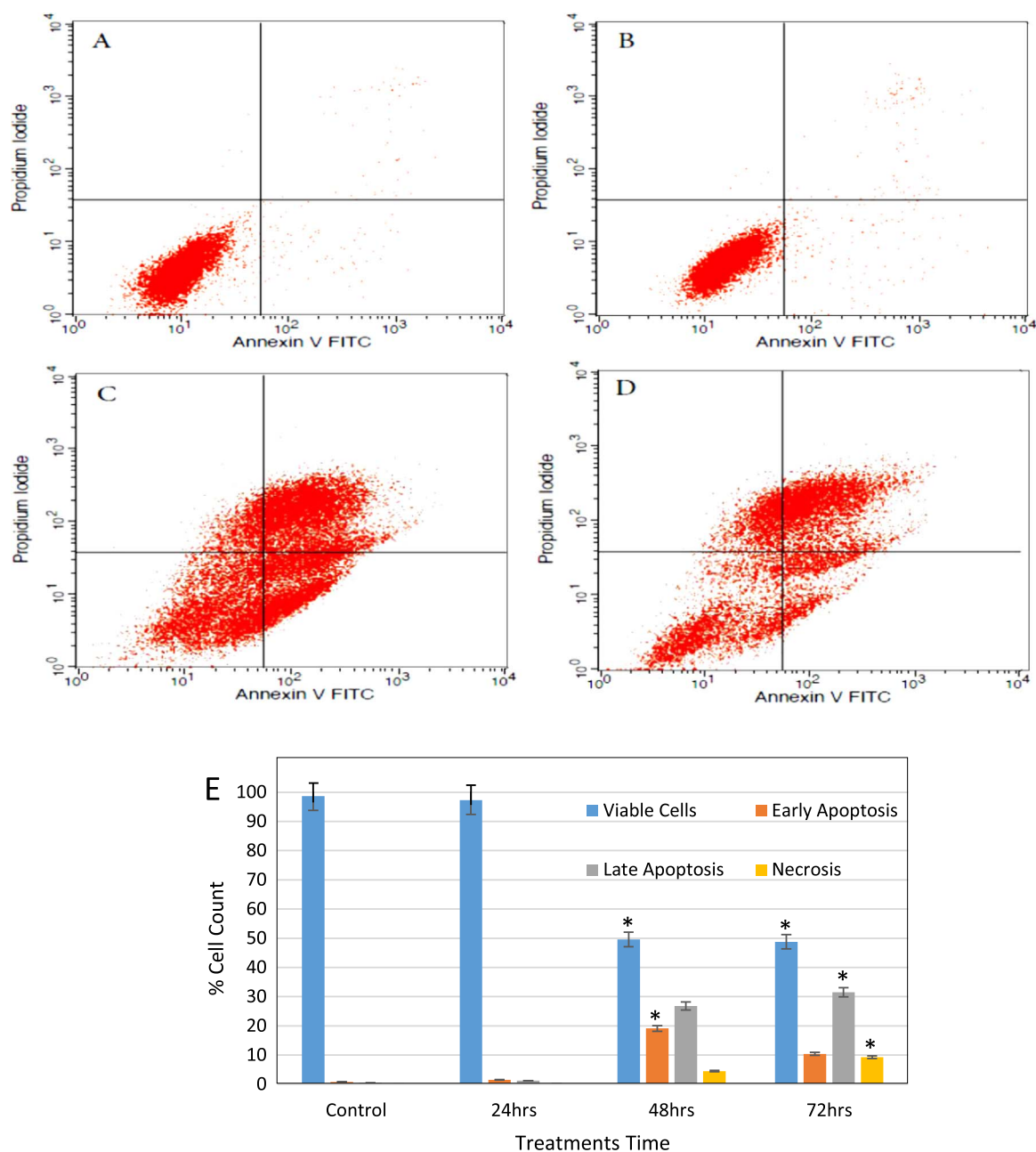
Fig. 7. Viability of hepG2 cells treated with 7.7 µg/mL clausenidin at (B) 24, (C) 48, and (D) 72 h, respectively. (A) Untreated control cells, (E) distribution of hepG2 cells according to viability in stages of cell death in the annexin V assay *For cell viability state, means significantly (p < 0.05) different from control.

3.9. Gene expression studies

There was significant (p < 0.05) increases in Apaf-1, JNK, cytochrome c, Bax, and caspases 3 and 9 gene expressions in hepG2 cells after treatment with clausenidin (Fig. 10A and B). Increases in bax and caspases 3 genes began at 12 h after clausenidin treatment.

3.10. Protein profile assay

Bax, cytochrome c, and cleaved caspase 3 protein expressions in hepG2 cells significantly (p < 0.05) increased with clausenidin treatment (Fig. 11). Conversely, Bcl-x, Bcl-2, and pro-caspase 3 protein expressions significantly (p < 0.05) decreased with treatment (Table 3).

4. Discussion

Several compounds from tropical plants have been shown to induce cancer cell toxicity either directly or by modulating cell biochemical pathways (Singh et al., 2003; Kintzios and Barberaki, 2004). In this study, we showed that clausenidin induced dose-dependent toxicity and apoptosis of hepG2 cells. We suspect that the effect of clausenidin is due to the presence of the two carbonyl groups in the pyranocoumarin rings of the compound. This is because most cytotoxic natural compounds appear to contain carbonyl groups in their basic structures. Besides, clausenidin, being a moderately sized molecule (Fig. 1), can easily enter tumor cells.

Apoptosis is the mode of cell death targeted in the development of anticancer compounds (Fesik, 2005). With that objective, we showed that anti-hepG2 cell effect of clausenidin is primarily through the induction of mitochondrial apoptotic pathway. The anticancer cell
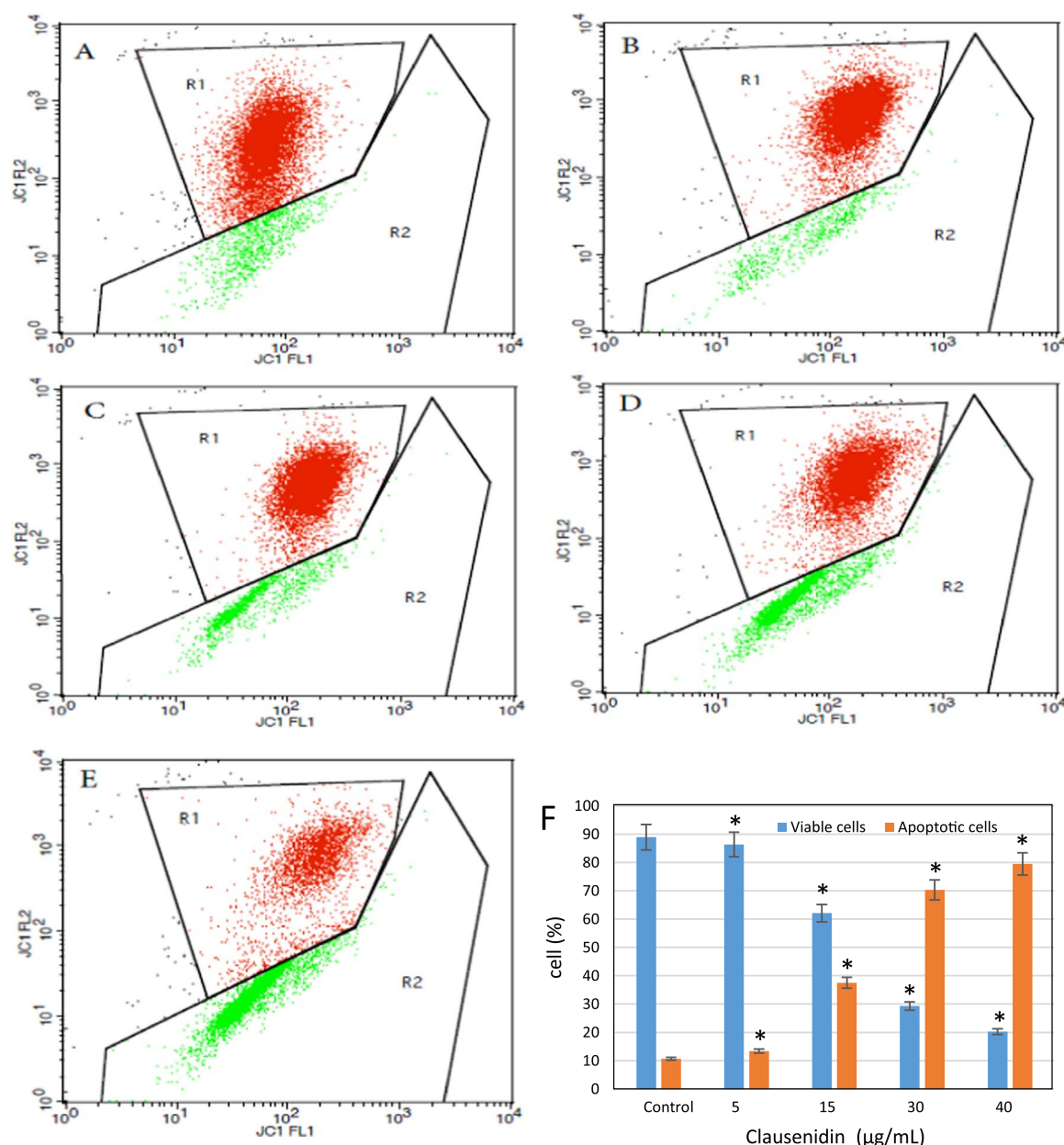
Fig. 8. HepG2 cell mitochondrial membrane depolarization after treatment with (B) 5, (C) 15, (D) 30, and (E) 40 μg/mL clausenidin. (A) Untreated control cells, (F) Viable and apoptotic clausenidin-treated cells. Red fluorescence=cells with intact/polarized mitochondria, Green fluorescence=cells with compromised/depolarized mitochondria. *For each cell type, means significantly (p < 0.05) different from control.
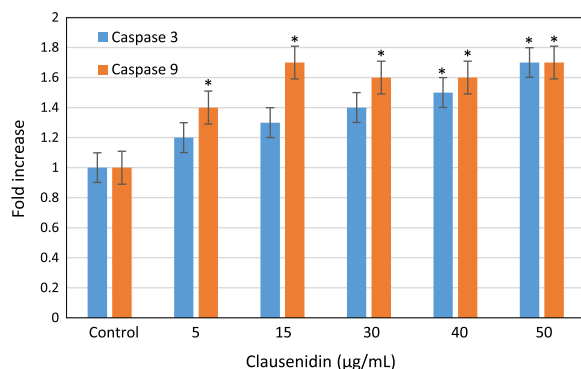

Fig. 9. Caspases 3 and 9 activities in hepG2 cells treated with clausenidin. *For each caspase, means significantly (p < 0.05) different from control.

effect increased with increase in clausenidin concentration. Most of the treated hepG2 cells showed the typical characteristics of apoptosis to include membrane blebbing, chromatin condensation, apoptotic body formation (Majno and Joris, 1995, Kroemer et al., 2005) However, a small percentage of clausenidin-treated hepG2 cells underwent necrosis.

Cell cycle regulation is an integral event for normal cell division (Mohan et al., 2010) while the induction of cell cycle arrest and apoptosis in cancer cells are hallmarks of anticancer drugs (Kummalue et al., 2007). Many natural compounds can trigger cell death through the modulation of the cell cycle (González-Sarrías et al., 2012). Our study reveals that clausenidin influenced the hepG2 cell cycle by causing growth arrest at the G2/M phase. There was also significant shift of treated hepG2 towards the G0/G1 phase that represents cells with fractioned DNA, the stage of the cycle, before the cells undergo actual apoptosis. Several pyranocoumarins to include nordentatin, clausarin and xanthoxyletin from the *Rutaceae* family inhibit cancer
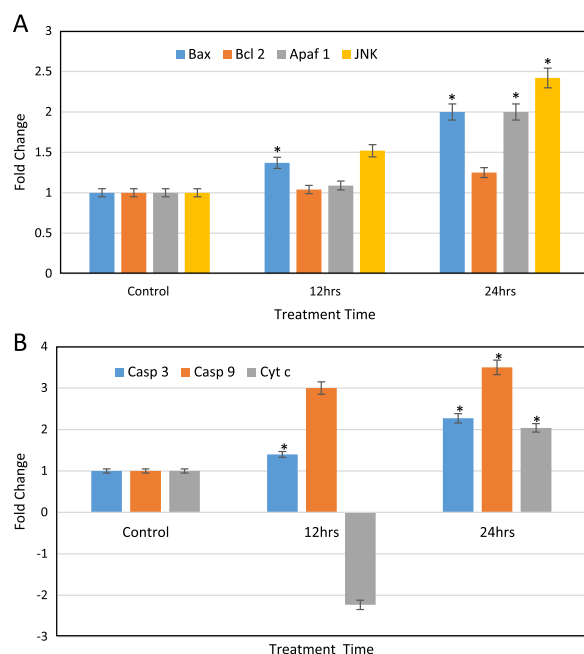
Fig. 10. Bax, Bcl-2, Apaf-1, JNK, caspase 3, caspase 9 and cytochrome c gene expressions in hepG2 cells treated with 7.7 µg/mL clausenidin. *For genes, means differ significantly (p < 0.05) from control.
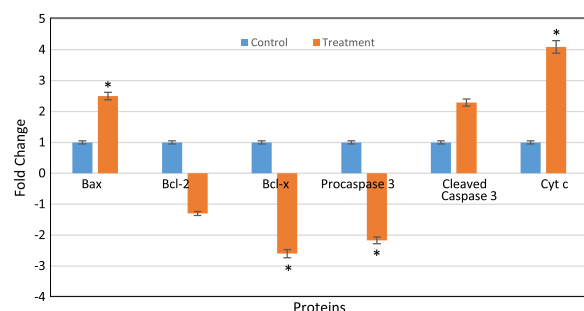

Fig. 11. Relative apoptotic protein expression in hepG2 cells treated with 7.7 µg/mL clausenidin for 24 h.

Table 3
Analysis of apoptosis related pathway proteins in clausenidin-treated hepG2 cells.

Proteins	Fold change	Regulation	Full name
Bad	2.77	Up	Bcl 2 associated death promoter
Bax	2.50	Up	Bcl-2 associated X protein
Bcl-2	−1.30	Down	B-cell lymphoma 2
Bcl-x	−2.60	Down	B-cell lymphoma x
Procaspase 3	−2.17	Down	Pro cysteine aspartic acid protease 3
Cleaved caspase 3	2.29	Up	Cleaved cysteine aspartic acid protease 3
Catalase	2.16	Up	Catalase
cIAP-1	1.87	Up	Cellular inhibitor of apoptosis 1
cIAP-2	2.12	Up	Cellular inhibitor of apoptosis 2
Claspin	1.86	Up	Claspin
Clusterin	1.38	Up	Clusterin
Cytochrome C	4.09	Up	Cytochrome C Complex

cell growth in similar manner (Su et al., 2009).

Clausenidin treatment had caused mitochondrial membrane depolarization of the hepG2 cells. Depolarization of the mitochondrial membrane is sine qua non for apoptosis to occur via the intrinsic pathway (Arbab et al., 2013). During apoptosis, mitochondrial membrane potential is frequently disrupted due to the formation of permeability transition pores or due to the insertion of pro-apoptotic proteins, such as bid or bax, in the mitochondrial membrane that prompts apoptosis (Zamzami and Kroemer, 2003). Clausenidin could have triggered the insertion of these pro-apoptotic proteins into the hepG2 mitochondrial membrane pores since the result of the proteins profile assay reveals significant increase in the expression of the pro-apoptotic proteins, Apaf-1, JNK, Bax, cyt c, with a concomitant decrease in the expression of the anti-apoptotic proteins, Bcl-2 and Bcl-x. The alteration in the fine balance between pro and anti-apoptotic proteins along with mitochondrial release of cytochrome c that subsequently activates caspases 3 and 9 result in apoptosis (Liu et al., 1996, Kluck et al., 1997, Yang et al., 1997, Jürgensmeier et al., 1998).

Most anticancer drugs induce apoptosis in cancer cells via the activation of cytochrome c/caspase 9 pathways or by affecting the mitochondrial membrane (Kaufmann and Earnshaw, 2000, Preston et al., 2001). This effect was observed with clausenidin on hepG2 cells. Clausenidin caused significant increase in the levels of caspases 3 and 9 in hepG2 cells. Caspase 3 is an executioner caspases of apoptosis, exerting its effect via selective destruction of subcellular structures, organelles or even the genome (Hanahan and Weinberg, 2000). Caspases are known to cleave different proteins in order to ensure the irreversibility of apoptosis (Fleischer et al., 2006). The elevation of caspases 9 and 3 levels as observed in this study strongly suggests that clausenidin-induced apoptosis is not only via stimulation of the mitochondria pathway but also involves destruction of cellular structures imperative for cell survival.

To further corroborate our findings, we conducted a gene expression studies and it was shown that clausenidin induces upregulation of pro-apoptotic Bax genes and a downward regulation of the anti-apoptotic Bcl-2 gene, which are consistent with equivalent expressions of the respective proteins. In the mitochondrial activated apoptosis, JNK is known to mediate in the interaction between Apaf-1 and cytochrome c to form the apoptosome complex that activates upstream and downstream caspases for eventual execution of apoptosis (Marsden et al., 2002). Clausenidin caused increased expression of the apoptosome complex genes, showing unequivocally the involvement of the mitochondria in its apoptotic effect on the hepG2 cells. The attempt by the hepG2 cells to induce expression of Bcl 2 gene to sufficiently block apoptosis was effectively prevented by clausenidin.

In conclusion, the study reveals that clausenidin is a potential alternative to existing drugs in the treatment of hepatocellular carcinoma. The anticancer effect of clausenidin is suggested to be multifaceted, by induction of intrinsic pathway of apoptosis and G2/M cell cycle arrest, formation of apoptosome complex, destruction of cell-maintenance organelles and structures, and obstructing cancer cell survival mechanisms.

Conflict of interest

The authors declare that there are no conflict(s) of interest pertaining this study.

Declaration

No part of the current report has been published elsewhere to the best of our knowledge. All.

Authors' have read and approved the manuscript for submission.

Contributions

List of authors and contributions to the study.

S/no	Author name	Contributions
1	Peter Waziri	Isolation of compound, experimental design, statistical analysis and preparation of manuscript.
2	Rasedee Abdullah	Experimental design, provided majority of all consumables used in the study as well as preparation of manuscript.
3	Swee Keong Yeap	Conducted the cell cycle assays, MMP assays, annexin V assays and preparation of manuscript.
4	Abdul Rahman Omar	Conducted the morphological analysis and preparation of the manuscript.
5	Ahmad Bustamam	Conducted the morphological analysis.
6	Nur Kartinee Kassim	Elucidation of the compound, clausenidin.
7	Ibrahim Malami	Conducted the statistical analysis.
8	Thiruventhan Karunakaran	Elucidation of the compound, clausenidin and preparation of the manuscript.
9	Mustapha Umar Imam	Conducted the gene expression studies.

Acknowledgement

References

Arbab, I.A., et al., 2013. Dentatin isolated from Clausena excavata induces apoptosis in MCF-7 cells through the intrinsic pathway with involvement of NF-κB signalling and G0/G1 cell cycle arrest: a bioassay-guided approach. J. Ethnopharmacol. 145 (1), 343–354.

Bakiri, L., Wagner, E.F., 2013. Mouse models for liver cancer. Mol. Oncol. 7 (2), 206–223.

Fahey, J.W., Stephenson, K.K., 2002. Pinostrobin from honey and Thai ginger (Boesenbergia pandurata): a potent flavonoid inducer of mammalian phase 2 chemoprotective and antioxidant enzymes. J. Agric. Food Chem. 50 (25), 7472–7476.

Ferlay, J., et al., 2010. Estimates of worldwide burden of cancer in 2008: globocan 2008. Int. J. Cancer 127 (12), 2893–2917.

Fesik, S.W., 2005. Promoting apoptosis as a strategy for cancer drug discovery. Nat. Rev. Cancer 5 (11), 876–885.

Fleischer, A., et al., 2006. Modulating apoptosis as a target for effective therapy. Mol. Immunol. 43 (8), 1065–1079.

González-Sarrías, A., et al., 2012. Anticancer effects of maple syrup phenolics and extracts on proliferation, apoptosis, and cell cycle arrest of human colon cells. J. Funct. Foods 4 (1), 185–196.

Hanahan, D., Weinberg, R.A., 2000. The hallmarks of cancer. Cell 100 (1), 57–70.

Huang, S.-C., et al., 1997. Two coumarins from the root bark of Clausena excavata. Phytochemistry 44 (1), 179–181.

Isa, N.M., et al., 2013. Boesenbergin A, a chalcone from Boesenbergia rotunda induces apoptosis via mitochondrial dysregulation and cytochrome c release in A549 cells in vitro: involvement of HSP70 and Bcl2/Bax signalling pathways. J. Funct. Foods 5 (1), 87–97.

Jing, L.J., et al., 2010. Phytochemicals, antioxidant properties and anticancer investigations of the different parts of several gingers species (Boesenbergia rotunda, Boesenbergia pulchella var attenuata and Boesenbergia armeniaca). J. Med. Plant Res. 4 (1), 27–32.

Jürgensmeier, J.M., et al., 1998. Bax directly induces release of cytochrome c from isolated mitochondria. Proc. Natl. Acad. Sci. 95 (9), 4997–5002.

Kaufmann, S.H., Earnshaw, W.C., 2000. Induction of apoptosis by cancer chemotherapy. Exp. Cell Res. 256 (1), 42–49.

Kintzios, S.E., Barberaki, M.G., 2004. Plants that Fight Cancer. CRC Press, London.

Kluck, R.M., et al., 1997. The release of cytochrome c from mitochondria: a primary site for Bcl-2 regulation of apoptosis. Science 275 (5303), 1132–1136.

Kongkathip, B., et al., 2005. Anti-HIV-1 constituents from Clausena excavata: part II. Carbazoles and a pyranocoumarin. Phytother. Res. 19 (8), 728–731.

Kroemer, G., et al., 2005. Classification of cell death: recommendations of the nomenclature committee on cell death. Cell Death Differ. 12, 1463–1467.

Kummalue, T., et al., 2007. Antiproliferative effect of Erycibe elliptilimba on human breast cancer cell lines. J. Ethnopharmacol. 110 (3), 439–443.

Liu, X., et al., 1996. Induction of apoptotic program in cell-free extracts: requirement for dATP and cytochrome c. Cell 86 (1), 147–157.

Majno, G., Joris, I., 1995. Apoptosis, oncosis, and necrosis. An overview of cell death. Am. J. Pathol. 146 (1), 3.

Manosroi, A., et al., 2004. Immunomodulatory activities of fractions from hot aqueous extract of wood from Clausena excavata. Fitoterapia 75 (3), 302–308.

Marsden, V.S., et al., 2002. Apoptosis initiated by Bcl-2-regulated caspase activation independently of the cytochrome c/Apaf-1/caspase-9 apoptosome. Nature 419 (6907), 634–637.

Mohan, S., et al., 2010. Typhonium flagelliforme induces apoptosis in CEMss cells via activation of caspase-9, PARP cleavage and cytochrome c release: its activation coupled with G0/G1 phase cell cycle arrest. J. Ethnopharmacol. 131 (3), 592–600.

Nordenstedt, H., et al., 2010. The changing pattern of epidemiology in hepatocellular carcinoma. Dig. Liver Dis. 42, S206–S214.

Perry, L.M., Metzger, J., 1980. Medicinal Plants of East and Southeast Asia: Attributed Properties and Uses. MIT Press, Cambridge Mass. & London, England.

Preston, T.J., et al., 2001. Mitochondrial contributions to cancer cell physiology: potential for drug development. Adv. Drug Deliv. Rev. 49 (1), 45–61.

Sharif, N.M., Mustahil, N.A., Noor, N,M, Sukari, M.A., Rahmani, M., Taufiq-Yap, Y.H., Ee, G.C.L., 2011. Cytotoxic constituents of Clausena excavata. Afr. J. Biotechnol. 10 (72), 16337–16341.

Singh, B., et al., 2003. Potential therapeutic applications of some antinutritional plant secondary metabolites. J. Agric. Food Chem. 51 (19), 5579–5597.

Su, C.-R., et al., 2009. Anti-HBV and cytotoxic activities of pyranocoumarin derivatives. Bioorg. Med. Chem. 17 (16), 6137–6143.

SyamaS., et al. 2013. b-Mangostin induces p53-dependent G2/M cell cycle arrest and apoptosis through ROS mediated mitochondrial pathway and NfkB suppression in MCF-7 cells.

Takemura, Y., et al., 2000. Four new furanone-coumarins from Clausena excavata. Chem. Pharm. Bull. 48 (4), 582–584.

Tuchinda, P., et al., 2002. Anti-inflammatory cyclohexenyl chalcone derivatives in Boesenbergia pandurata. Phytochemistry 59 (2), 169–173.

WHO (World Health Organization), 2015. Cancer Fact Sheet. ⟨http://www.who.int/mediacentre/factsheets/fs297/en/⟩ (accessed on 25.09.16)

Wu, C.-C., et al., 1994. Antiplatelet effects of clausine-D isolated from Clausena excavata. Biochim. Biophys. Acta – Gen. Subj. 1201 (1), 1–6.

Wu, T.-S., Furukawa, H., 1982. Biological and phytochemical investigation of Clausena excavata. J. Nat. Prod. 45 (6), 718–720.

Yang, J., et al., 1997. Prevention of apoptosis by Bcl-2: release of cytochrome c from mitochondria blocked. Science 275 (5303), 1129–1132.

Yun, J.-M., et al., 2006. Induction of apoptosis and cell cycle arrest by a chalcone panduratin A isolated from Kaempferia pandurata in androgen-independent human prostate cancer cells PC3 and DU145. Carcinogenesis 27 (7), 1454–1464.

Zamzami, N., Kroemer, G., 2003. Apoptosis: mitochondrial membrane permeabilization – the (w) hole story? Curr. Biol. 13 (2), R71–R73.

Zhang, J., et al., 2014. Chemopreventive effect of flavonoids from Ougan (Citrus reticulata cv. Suavissima) fruit against cancer cell proliferation and migration. J. Funct. Foods 10, 511–519.